

Airbrush-Spray Deposition of Colloidal Polymer Films

Sascha Prommegger

Supervised by
Dr. Stephan V. Roth

Abstract:

The technique of airbrush-spray deposition was used to create thin films of nanoparticles on a flat surface. The dependence of the film formation on the concentration of the particles was investigated using grazing-incidence small-angle X-ray scattering as well as optical microscopy.

1. Introduction

The aim of this project was to investigate the formation of films of nanoparticles in solution on a flat surface via airbrush spray deposition and their dependence on the concentration, size and surface structure of the particles. For this, optical microscopy and grazing-incidence small-angle X-ray scattering (GISAXS) were used at the microfocus and nanofocus X-ray scattering beamline situated at the PETRA III positron storage ring at DESY (Deutsches Elektronen-Synchrotron).

The GISAXS method is particularly well suited to investigate films on top of a substrate as it is very surface sensitive.

Spray deposition is a very important method to produce thin films of nanoparticles as it allows to get very homogeneous films over larger areas in a very short time. This is important for many applications, for example for solar cells. Compared to other techniques like dip-coating, solution casting, inkjet printing or vacuum deposition the airbrush-spray method has only been developed recently and has not been investigated so thoroughly.

2. Sample Preparation

For spraying the solutions a commercially available airbrush spray device from Harder and Steenbeck was used (Figure 1). The device was mounted above the substrate to spray vertically downwards from adjustable distance. As a propellant Argon gas was used.

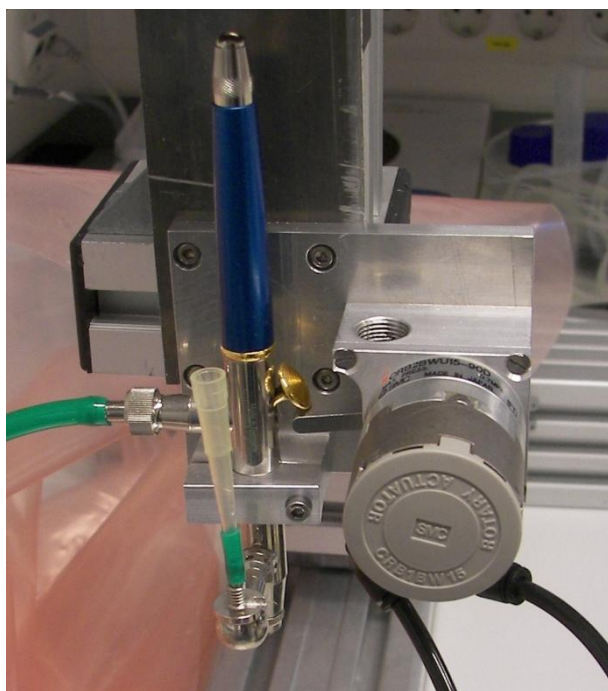


Figure 1: The spray device. The spraying solution was inserted through the pipette tip. A motor, controlled via pressurised air, was used to switch the device on and off. The substrate was mounted below the device.

The colloids used were polystyrene with two different particle sizes, 100 nm and 200 nm, each with two different surfaces, plain and carboxylated. Each of the four particle types were sprayed in a series of concentrations between 0.25 mg/ml (1%) and 25 mg/ml (100%), diluted with ethanol, at a substrate distance of 10 cm, Argon pressure of 1 bar and a spray duration of 0.1 seconds.

As substrate microscopy glass plates were used, cleaned in an acidic bath to give better wetting properties and prevent the formation of droplets.

Besides the effect of varying concentration the dependence on spraying distance and Argon pressure were also investigated using the 200 nm plain polystyrene at 15% concentration. The distance was varied between 5, 10 and 15 cm at constant pressure and the pressure was varied between 1 and 5 bar in steps of 1 bar at constant distance.

For the 5 cm distance the spray time had to be reduced by half in order to not get too much liquid on the limited size of the substrate.

3. Optical Microscopy

The KEYANCE digital microscope VHX-600 was used for optical investigation of the samples with magnifications of 250 and 2500 times.

The plain polystyrene colloids with 200 nm at a very low concentration of 1% showed individual particles at a distance of several micrometres. Their size was measured as 500 nm using a measuring function of the microscope. To distinguish whether these objects are several nanoparticles clustered together or the individual particles appear larger due to optical effects is beyond the resolution limitations of the optical microscope.

At concentrations between 5% and 20% these particles formed a closed thin film. At 35% and 50% increasingly large clusters appeared on top of the film. At 75% and 100% the film became thicker and colours appeared (Figure 2).

In the carboxylated case the particles appeared slightly larger than for the plain polystyrene (Figure 3). At 10% concentration larger, cone-like structures begin to form on top of the thin film (Figure 4).

For 100 nm sized colloids the individual particles can barely be seen.

Concerning the pressure variation no significant difference could be seen at pressures between 1 and 4 bar. At 5 bar the film became a bit less homogeneous.

No difference was observed for varying spray distance.

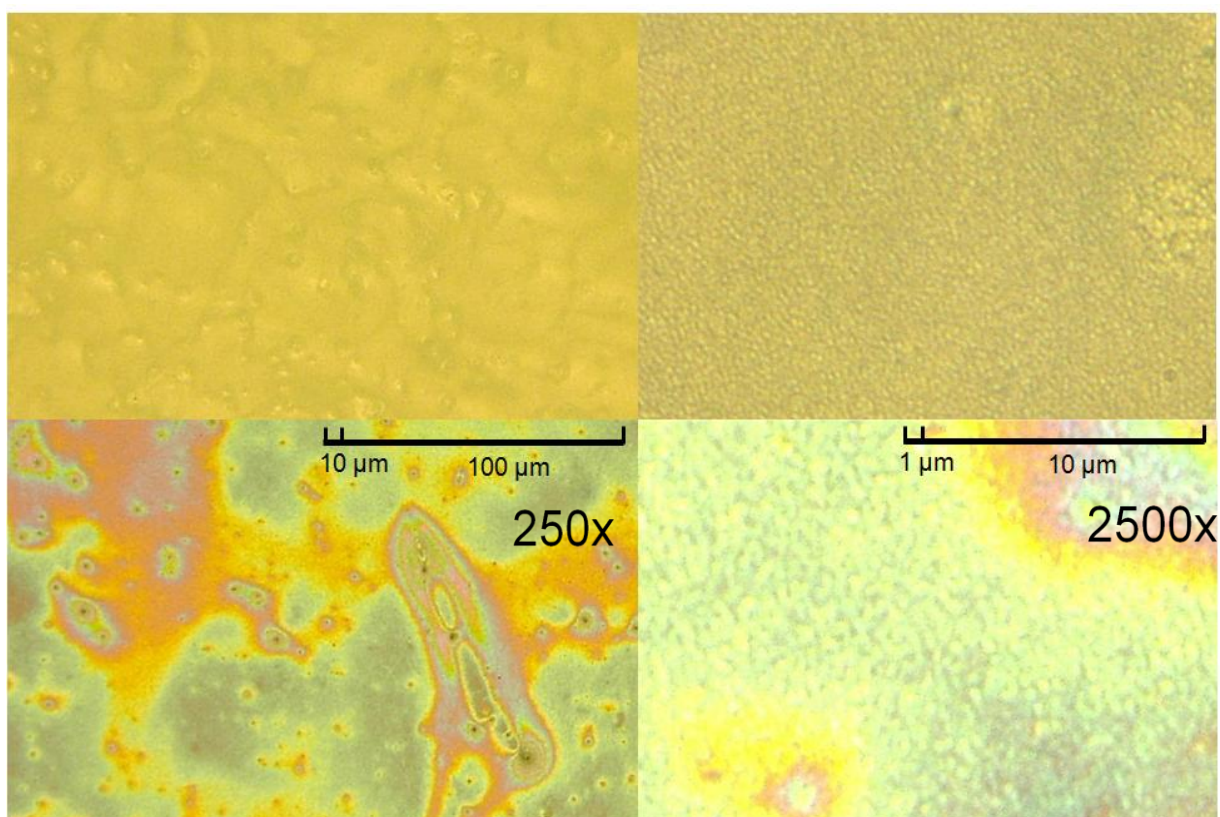


Figure 2: 200 nm plain polystyrene at 20% concentration (top) and 75% concentration (bottom) at 250x (left) and 2500x (right) magnification. At 20% a thin film of the individual nanoparticles can be seen whereas at 75% a thick film has formed.

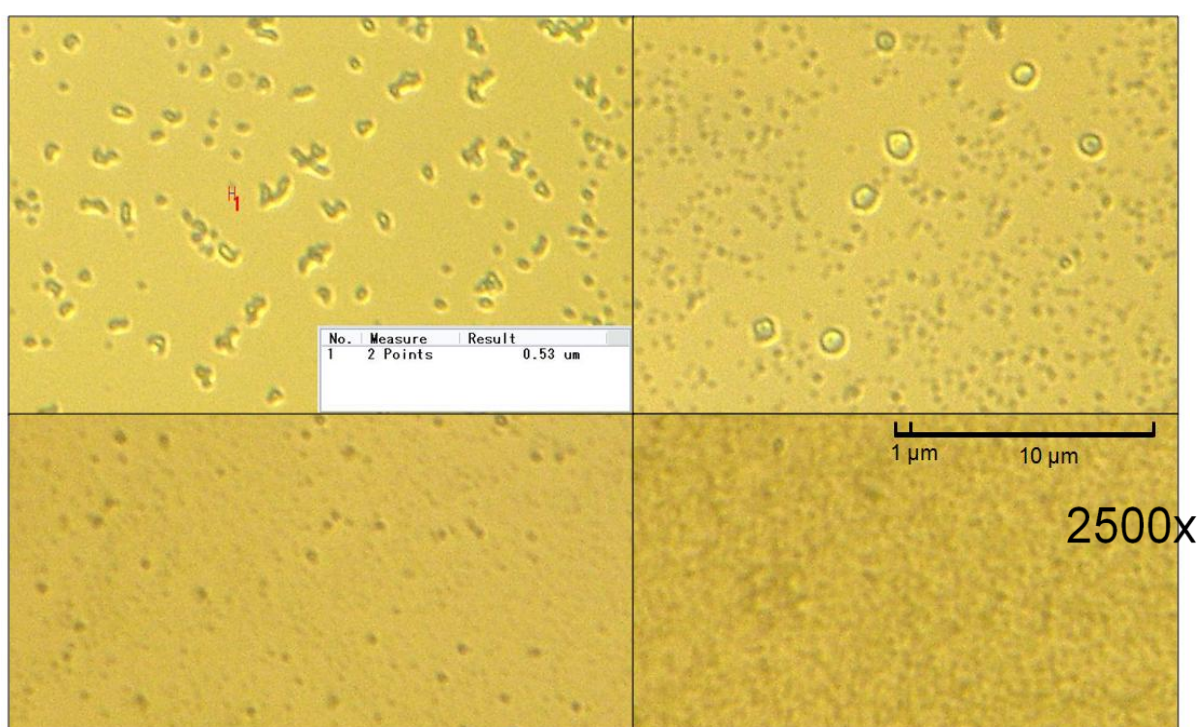


Figure 3: Plain polystyrene at 1% concentration (left) and carboxylated polystyrene at 2% (right) with particle size of 200 nm (top) and 100 nm (bottom). The first picture shows an individual particle measured with the microscope as 500 nm.

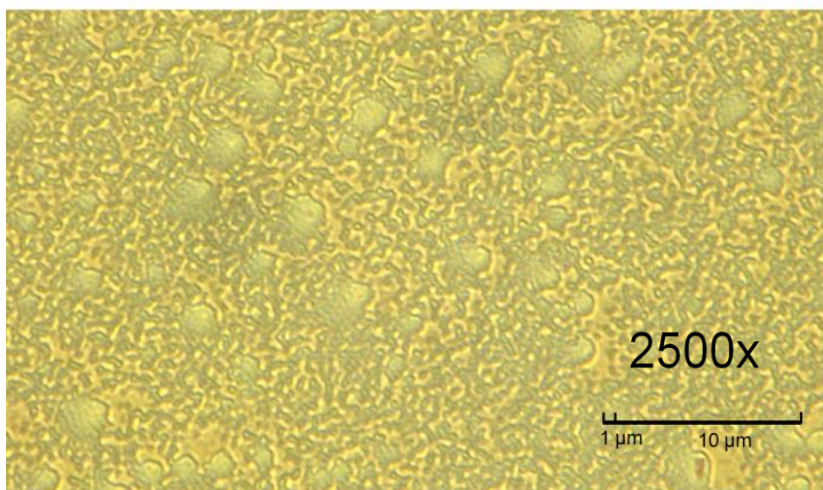


Figure 4: Formation of cone-like structures on top of the thin film for carboxylated polystyrene at 30% concentration.

4. Measuring with the beam

The measurements were done with an X-ray beam of 0.957 \AA . Each sample had first to be aligned to be hit by the beam at the right position and angle. For the alignment a diode was used to measure the intensity of the beam after it passed the sample. Three steps of alignment were:

- To find the correct z-position (height) of the sample so that it is half in the beam. This was simply done by scanning along the z-axis to find the position with half the intensity of the incoming beam. Due to the top-up mode of the PETRA III storage ring the beam intensity is constant in time which makes this process faster.
- To find the zero position of the incident beam angle a scan through the angle was made. At the correct zero position of the angle a sharp peak in intensity was measured with a maximum of half the incident beam intensity.
- The z-position of the sample for half maximum intensity was measured at two points along the y-axis (perpendicular to the beam). From that difference and the distance in y position the tilt of the sample could be measured and eliminated.

The sample was then investigated with the Pilatus detector.

Due to limited time only 5 different samples were measured: plain polystyrene with 200 nm diameter at 75% (18.75 mg/ml) concentration and with 100 nm diameter at 100% (25 mg/ml), 50% (12.5 mg/ml) and 10% (2.5 mg/ml) as well as carboxylated polystyrene with 100 nm at 100% (25 mg/ml). These will be denoted in the further text as pPS200-75, pPS100-100, pPS100-50, pPS100-10 and cPS100-100, respectively.

As the resolution on the detector image of the first sample (200 nm) was not very good, due to a short sample-detector distance, for the remaining measurements only samples from 100 nm particles were used which can be resolved more easily.

The incident beam angle was for the first sample (pPS200-75) at 0.5°. To get a better surface sensitivity it was decreased to 0.4° for the next two samples (pPS100-100 and cPS100-100) and further to 0.3° for the last two samples (pPS100-50 and pPS100-10) as shown in Table 1.

Each sample was scanned in detail over a distance of 16 mm along the y-direction (perpendicular to the beam). Table 1 shows the distance between two measuring positions in each scan, the resulting number of images, the incident angle and the exposure time.

Table 1: Distance between two scan positions, number of images per scan, incident beam angle and exposure time per image for the different samples investigated.

Sample	Scan steps (μm)	Number of images	Incident angle	Exposure time (s)
pPS200-75	2000	9	0.5°	3
pPS100-100	25	641	0.4°	1
cPS100-100	100	161	0.4°	5
pPS100-50	100	161	0.3°	3
pPS100-10	100	161	0.3°	3

5. Analysis

5.1. Out-of-Plane Cuts

The resulting detector images were analysed with the program DPDAK by making out-of-plane cuts at three different positions: horizontal through the Yoneda peak (cut 1) and through the specular peak (cut 2) and a central vertical cut (cut 3). A typical detector image and the cut positions are shown in Figure 5. All cuts had a width of 10 pixels. The position of the horizontal cuts varied between the different samples as the incident angle changed. An example for each of the cuts is shown in Figures 6-8.

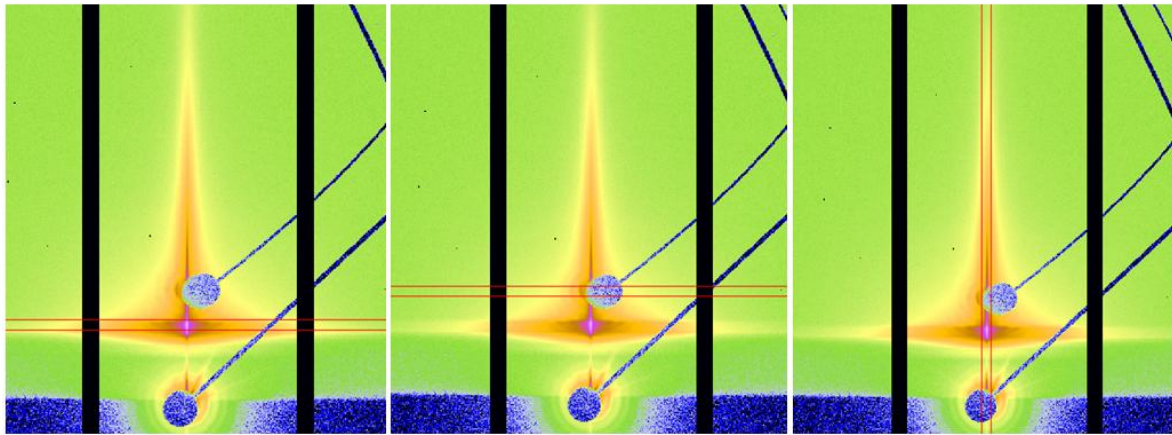
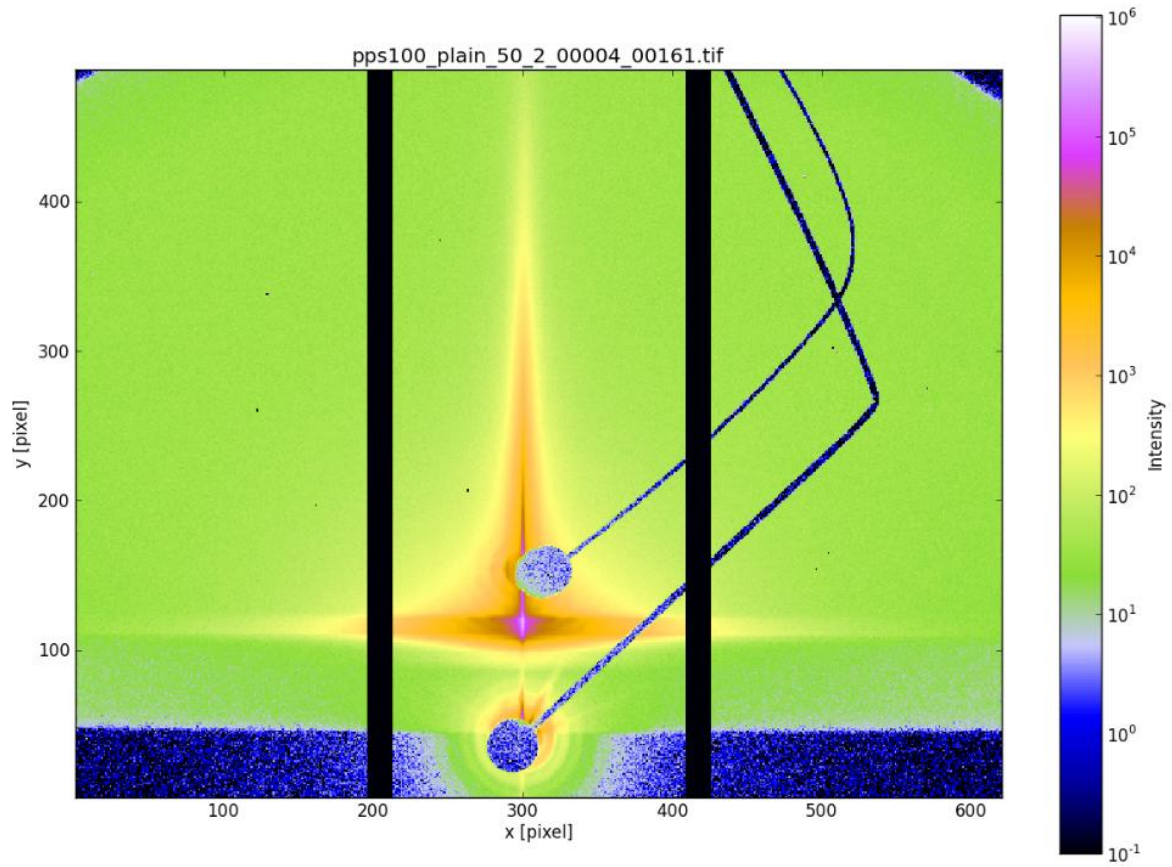


Figure 5: Top: Typical detector image (sample pPS100-50). Bottom: Positions of the out-of-plane cuts. The 3 cuts are horizontal through the Yoneda peak and through the specular peak and vertical through the centre.

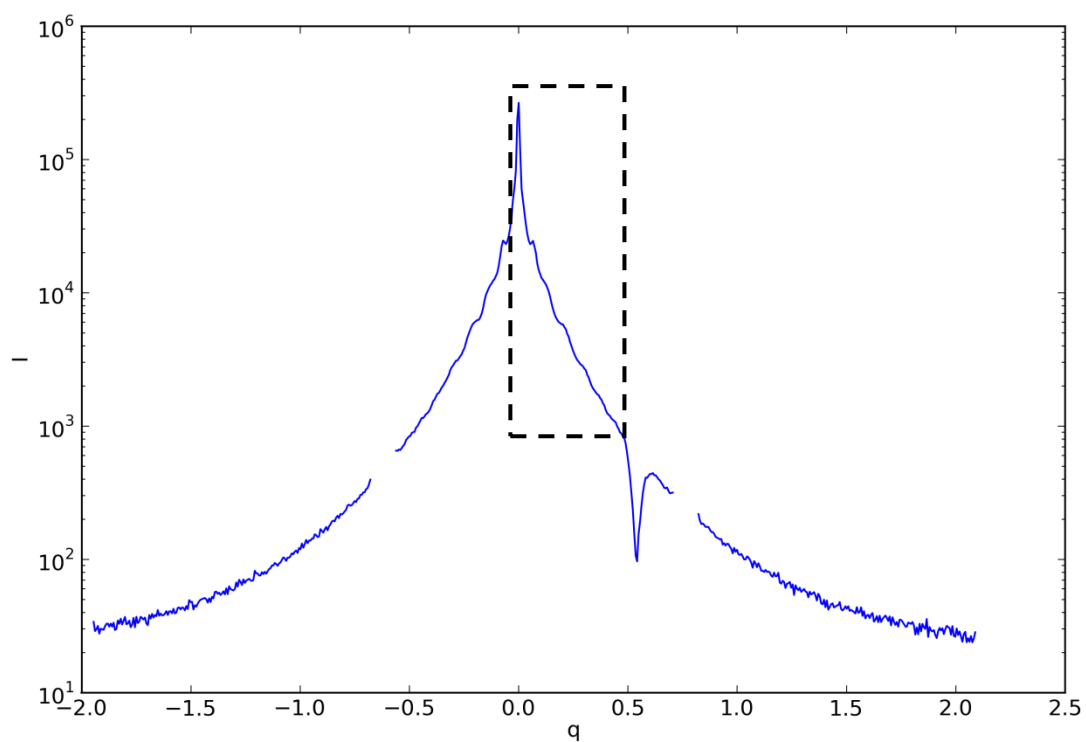


Figure 6: Cut 1 through the Yoneda peak (sample pPS100-50). The dashed line indicates the magnified section for the peak fits. The two gaps to either side are where the segments of the detector meet. The minimum at 0.5 q comes from the holder of the primary beamstop as can be seen in Figure 5.

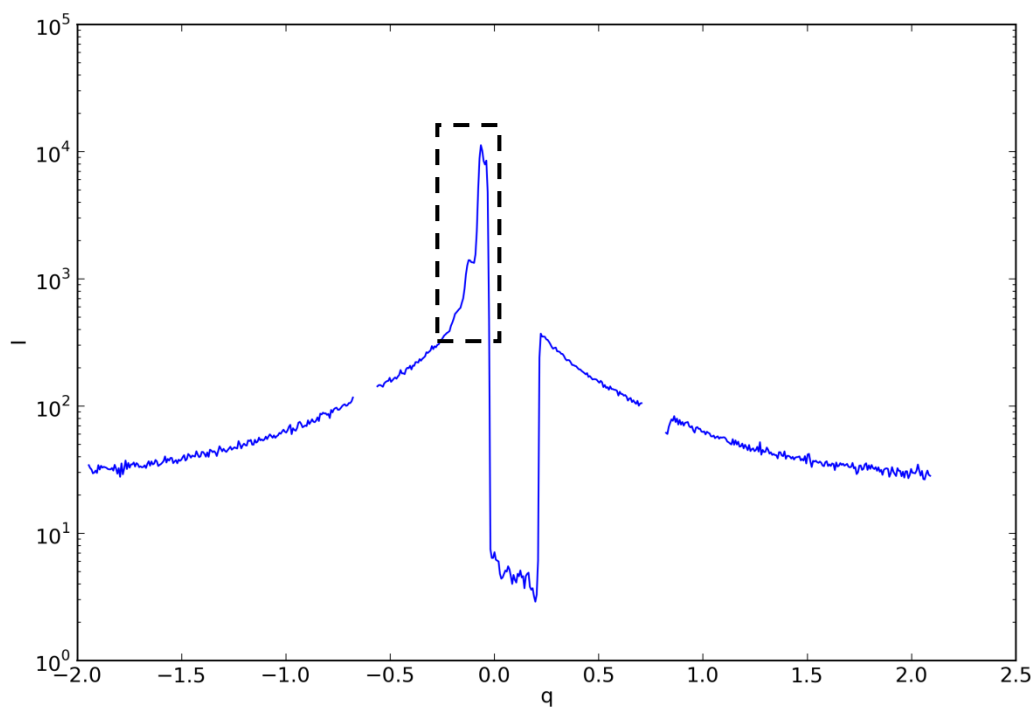


Figure 7: Cut 2 through the specular peak (sample pPS100-50). The dashed line indicates the magnified section for the peak fit. The gap in the centre comes from the specular beamstop.

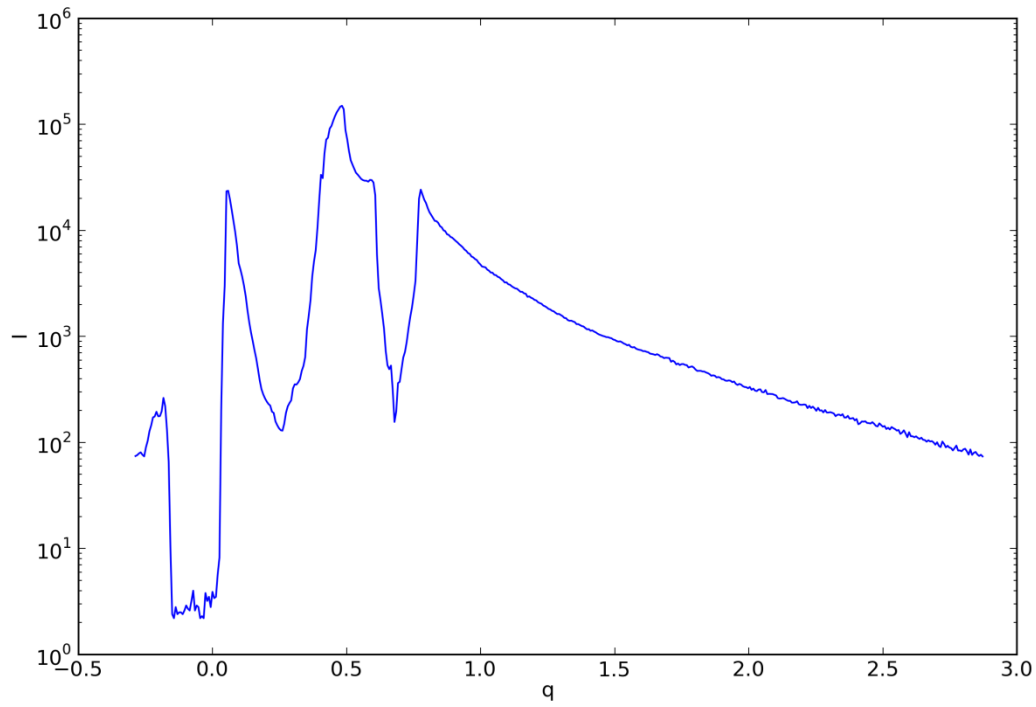


Figure 8: Cut 3 (vertical, sample pPS100-50). The maximum in the middle is the Yoneda peak. The minima on the left and on the right are due to the two beamstops. The minimum to the left of the Yoneda peak is real.

5.2. Homogeneity

Plotting cuts for all images of a scan on one graph allows to investigate the homogeneity of the sample. The position of discrepancies can be seen easily. All samples were found to be very homogeneous and showed only very localised irregularities (over a few images). An examples are shown in Figures 9 and 10.

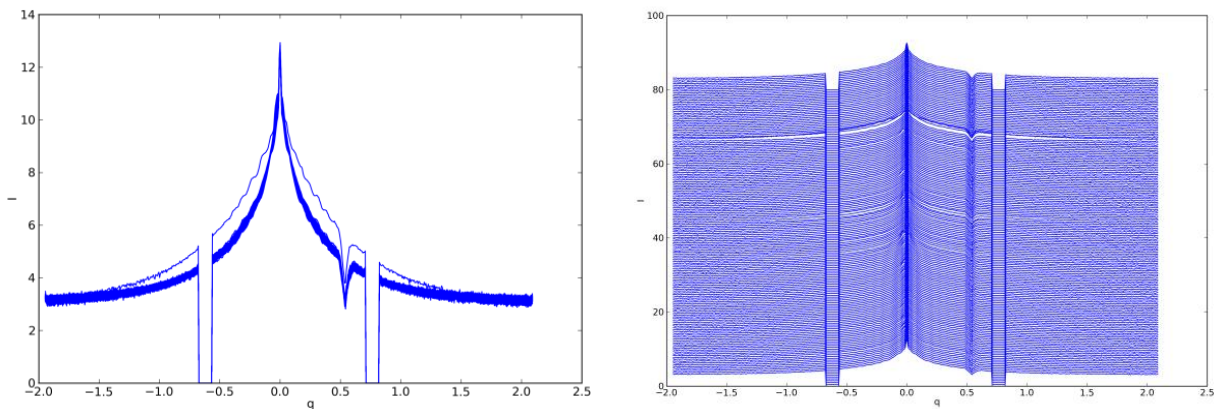


Figure 9: Cuts of all individual images in one scan plotted on one graph without (left) and with (right) each line displaced with respect to the previous. Amount and position of inhomogeneities can be found this way. (Example is pPS100-10, cut 1.)

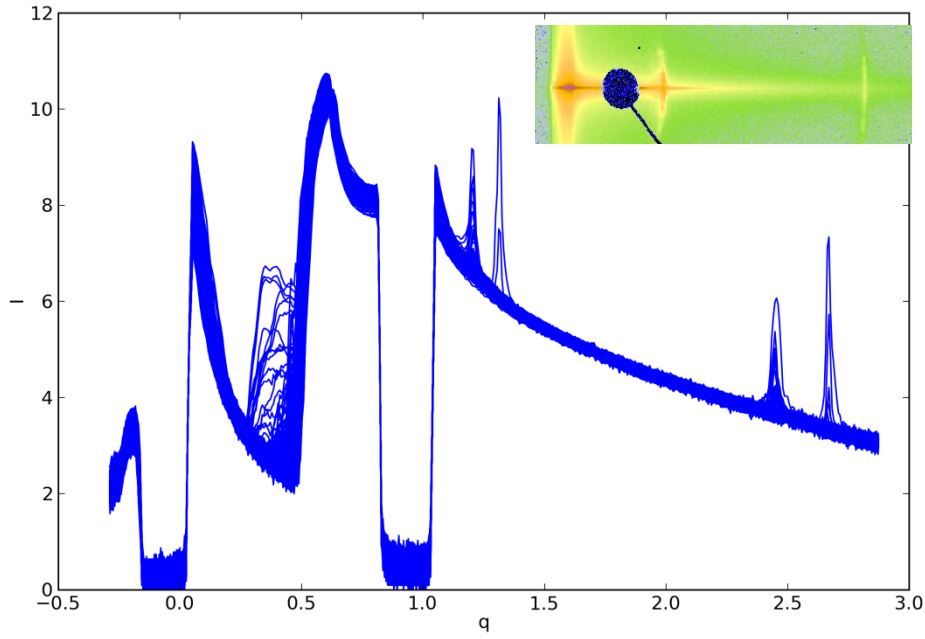


Figure 10: Most (local) inhomogeneities were observed in the vertical cut. The detector image (top right corner) shows the peaks that occasionally occur to the right of the beamstop. (pPS100-100, cut 3)

5.3. Peak Fits

5.3.1. Cut 1 – Yoneda peak

The cut through the Yoneda peak was fitted with Lorentzian peaks for the plain polystyrene samples. All samples show a first order side maximum and some of them show higher order side maxima. The first order side maximum is related to the size of the closely packed nanoparticles which can be found from its position with the formula $d = 2\pi/q$, where d is the diameter of the particles and q is the position of the peak in q -space. The positions of the peaks and the corresponding distances in real space for the different samples are shown in Table 2. To get a good fit with the central maximum it was also necessary to add an additional peak between the position of the central maximum and the first side maximum.

The higher order peaks come from the structure factor and their presence indicates a strong lateral ordering of the nanoparticles.

The fits for the cut through the Yoneda peak for the plain polystyrene samples are shown in Figures 11-14. The arrows indicate the position of the side maxima. The fit parameters of the first order maximum for each of the samples are shown in Table 3.

The average distance in real space found from the positions of the first order side maxima of the 100nm samples is 91 ± 9 nm. For the 200 nm colloids as distance of 188 ± 34 nm was found. The additional peaks near the central maximum give a distance of 250 ± 50 nm (for 100 nm colloids) and 275 ± 70 (for 200 nm colloids) in real space.

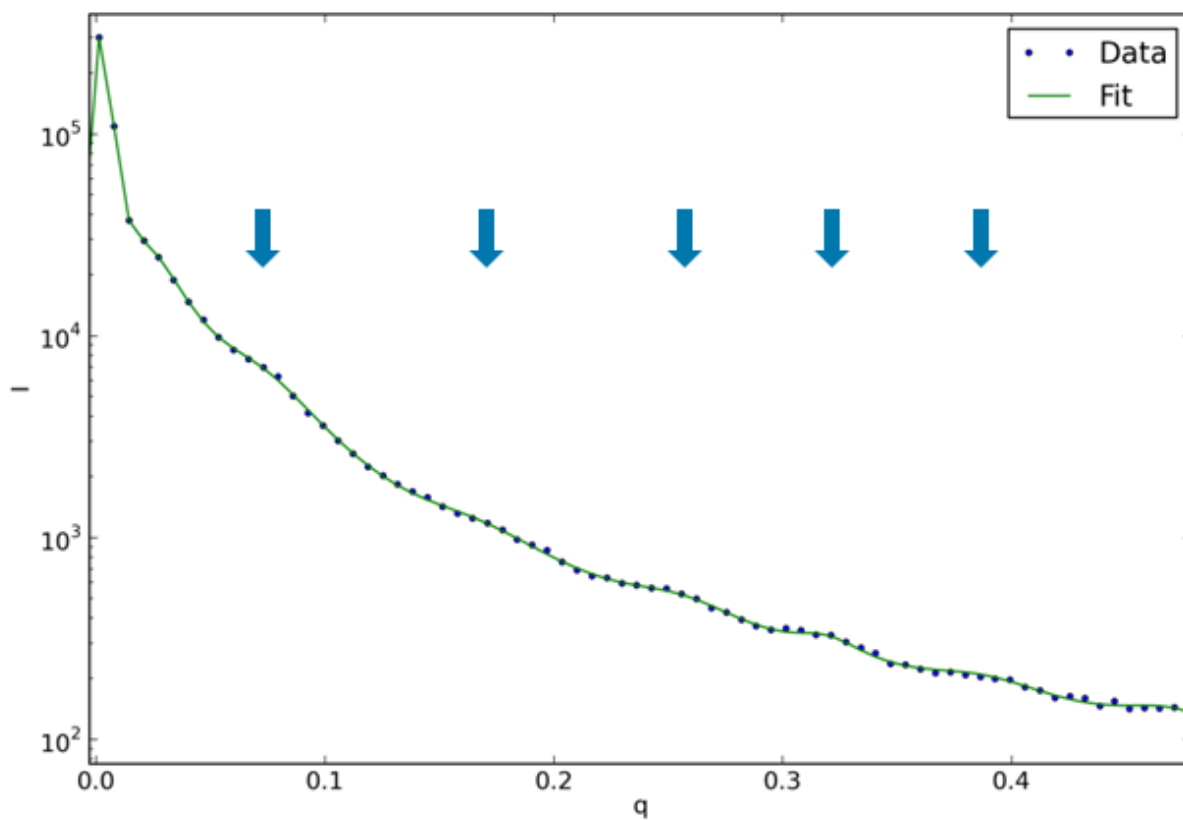


Figure 11: Cut 1 for pPS100-10. The arrows indicate the positions of the side maxima.

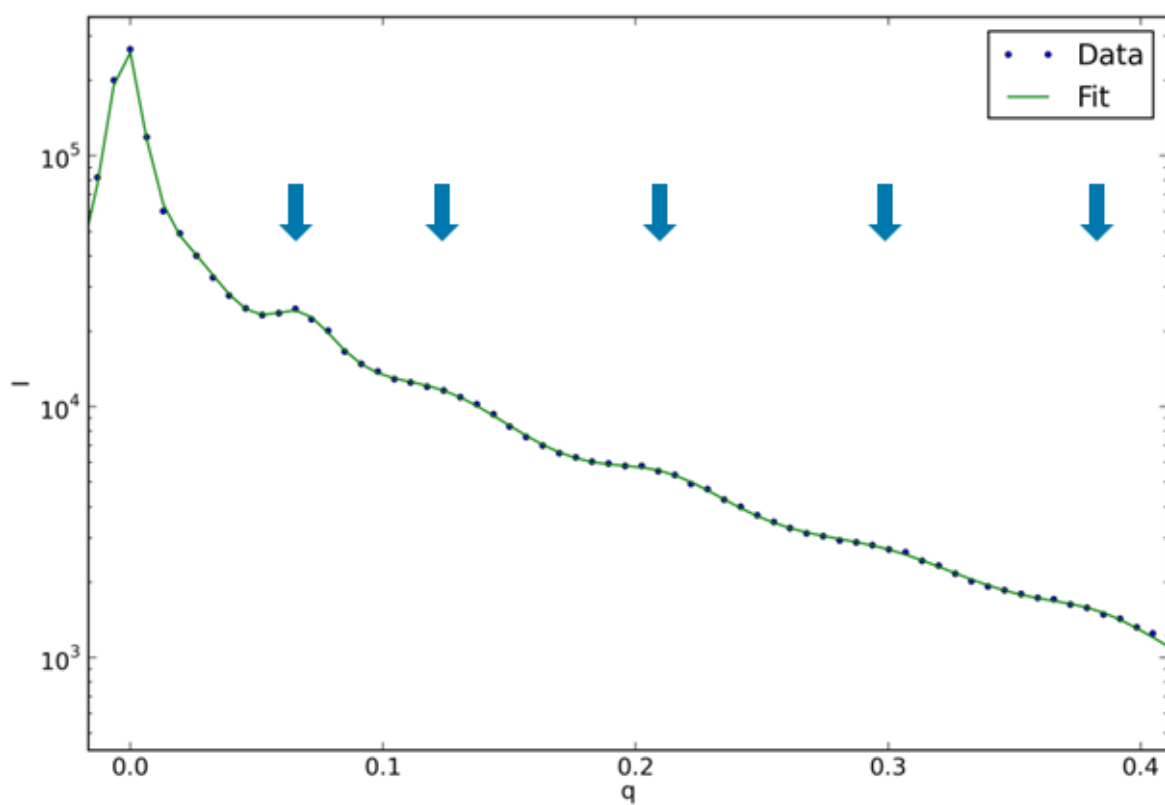


Figure 12: Cut 1 for pPS100-50.

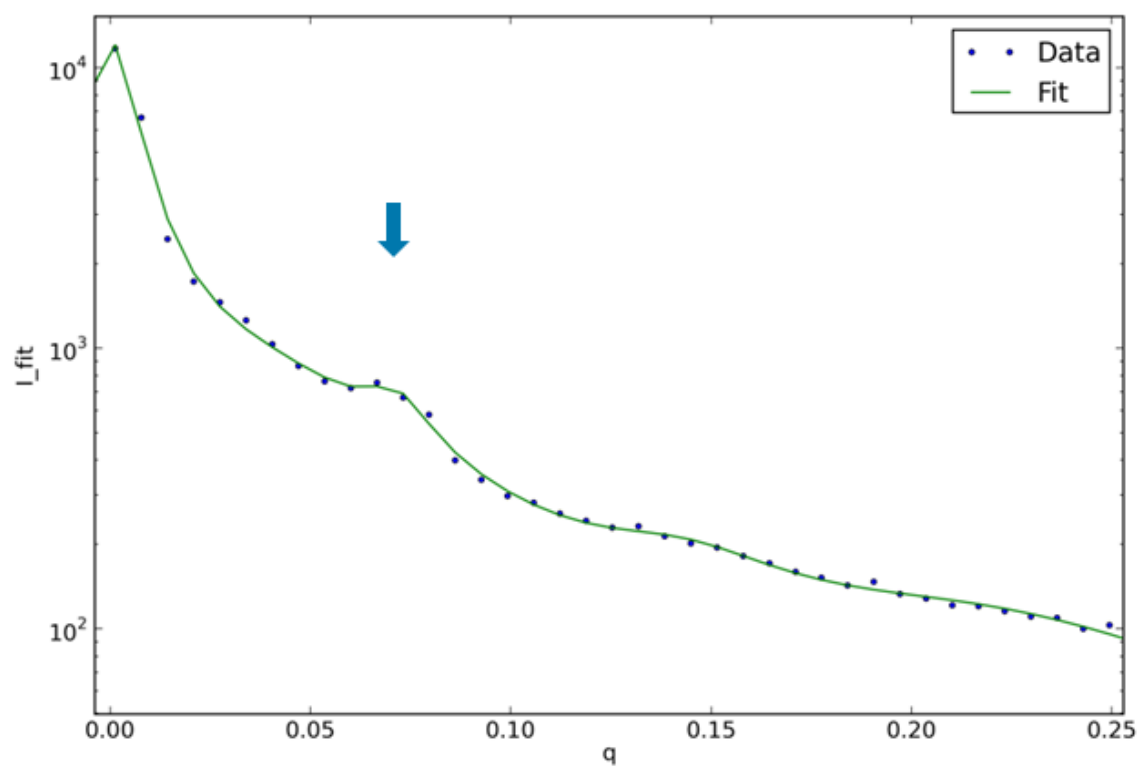


Figure 13: Cut 1 for pPS100-100. There are no clear higher order maxima.

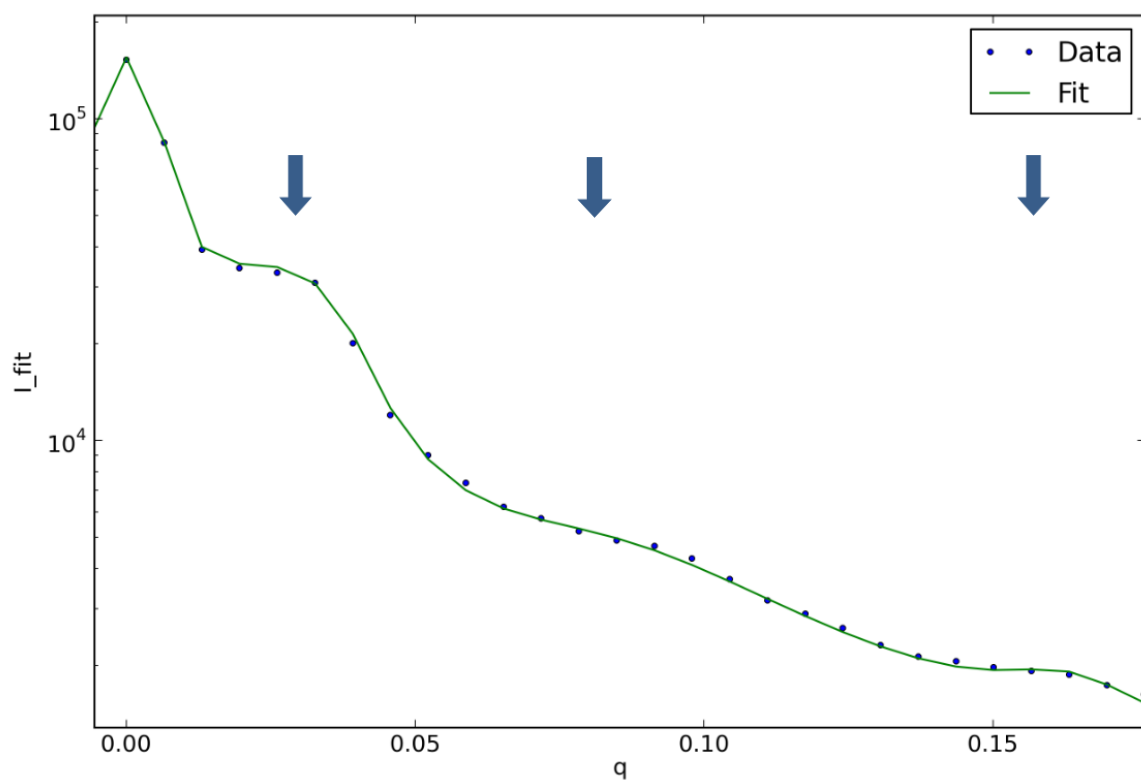


Figure 14: Cut 1 for pPS200-75.

Table 2: Side maxima positions in q-space and the corresponding distance in real space for cut 1 (through Yoneda peak) for the plain polystyrene samples. The 0th order peak is the additional peak that was necessary to fit the central maximum correctly.

	peak order	pPS100-10	pPS100-50	pPS100-100	pPS200-75
q-space (1/nm)	0	0.021 ± 0.006	0.023 ± 0.006	0.031 ± 0.006	0.023 ± 0.006
	1	0.069 ± 0.006	0.067 ± 0.006	0.071 ± 0.008	0.033 ± 0.006
	2	0.164 ± 0.006	0.120 ± 0.001	0.140 ± 0.080	0.081 ± 0.006
	3	0.254 ± 0.014	0.210 ± 0.002	0.200 ± 0.300	0.163 ± 0.017
	4	0.319 ± 0.018	0.295 ± 0.007		
	5	0.387 ± 0.037	0.381 ± 0.010		
real space (nm)	0	299.2 ± 85.5	273.2 ± 71.3	202.7 ± 39.2	275.4 ± 72.4
	1	91.1 ± 7.9	93.8 ± 8.4	88.5 ± 10.0	188.4 ± 33.9
	2	38.3 ± 1.4	52.4 ± 0.4	44.9 ± 25.6	77.3 ± 5.7
	3	24.7 ± 1.4	29.9 ± 0.3	31.4 ± 47.1	38.5 ± 4.0
	4	19.7 ± 1.1	21.3 ± 0.5		
	5	16.2 ± 1.6	16.5 ± 0.4		

Table 3: Peak parameters for the first order side maximum of the different samples.

sample	position (1/nm)	height (counts)	width (1/nm)
pPS100-10	6.86E-02 ± 1.27E-03	3.68E+03 ± 2.08E+02	6.35E-02 ± 4.10E-03
pPS100-50	6.74E-02 ± 1.82E-04	1.32E+04 ± 2.77E+02	3.83E-02 ± 1.11E-03
pPS100-100	7.11E-02 ± 7.93E-03	2.31E+02 ± 2.98E+02	1.93E-02 ± 4.48E-02
pPS200-75	3.33E-02 ± 4.30E-04	2.12E+04 ± 3.35E+02	1.70E-02 ± 2.82E-03

5.3.2. Cut 2 – specular peak

For the cuts through the specular peak a good fit was only achieved when using Gaussian curves for the side Maxima, but still a Lorentzian for the central maximum. The height and width of the latter had to be guessed as the actual peak was covered by the beamstop. For technical reasons the detector image was inverted so that the peaks positions had positive values. The fit is shown in Figure 15 and the fit parameters in Table 4.

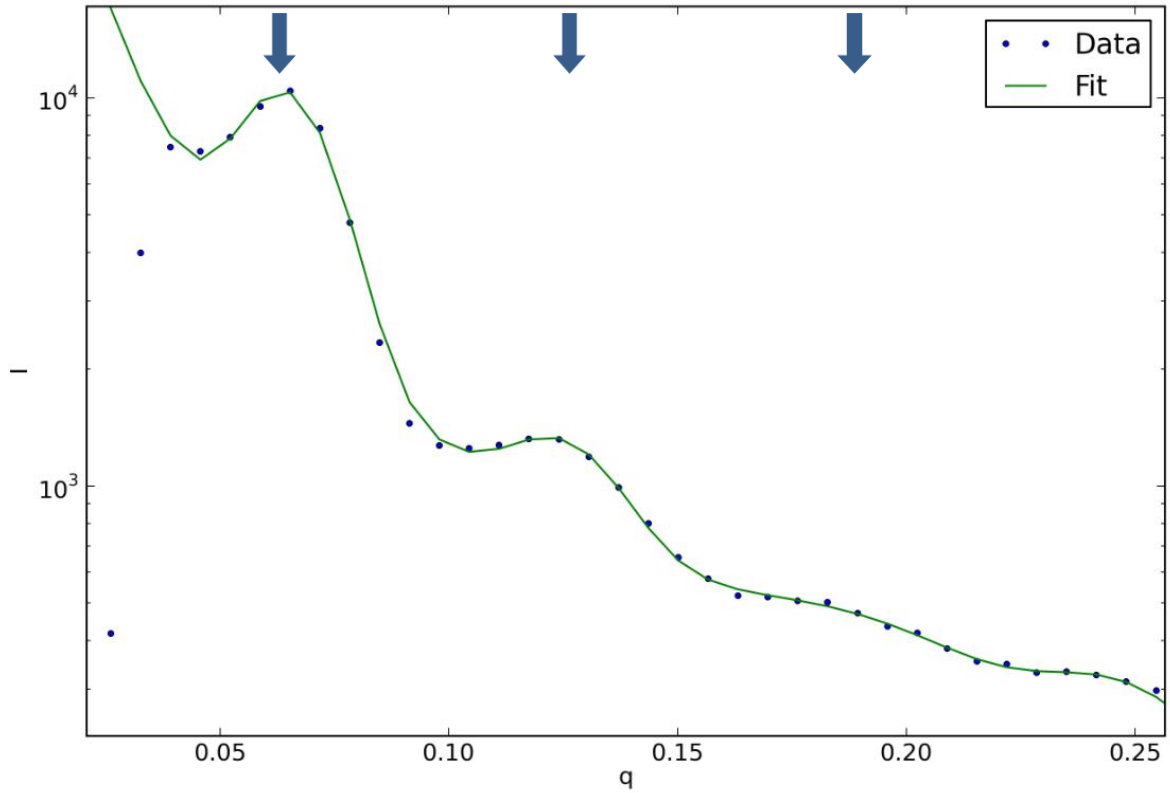


Figure 15: Cut 2 for pPS100-50. The picture was inverted before fitting to have the peaks on the positive side. The drop in intensity on the left is due to the beamstop.

Table 4: Side maxima positions in q-space and the corresponding distance in real space for cut 2 (through specular peak) for pPS100-50.

	peak order	pPS100-50
q space (1/nm)	1	0,065 ± 0,006
	2	0,125 ± 0,008
	3	0,188 ± 0,045
real space (nm)	1	97,3 ± 9,0
	2	50,2 ± 3,2
	3	33,4 ± 8,0

5.4. Structure Factor

To find the structure factor, the resulting fit was divided by the square of the form factor of a sphere with size of the nanoparticles. The form factor is given by

$$F(q) = A * \frac{\sin(qR) - qR \cos(qR)}{(qR)^3}$$

where R is the radius of the nanoparticle and A is a constant chosen in such a way that the first side maximum of the form factor and the fit have the same height (Figure 16). Figure 17 shows the resulting structure factor for the sample pPS100-50.

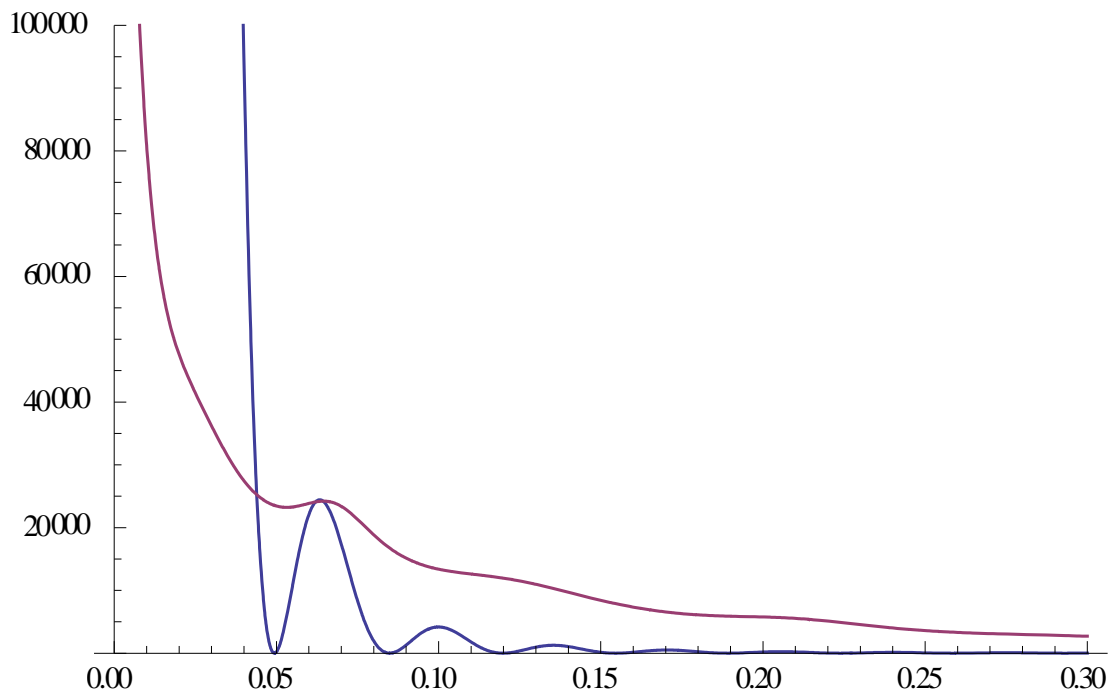


Figure 16: Peak fit (red) and form factor (blue). The height of the form factor was chosen so that the first side maxima of the two curves have the height.

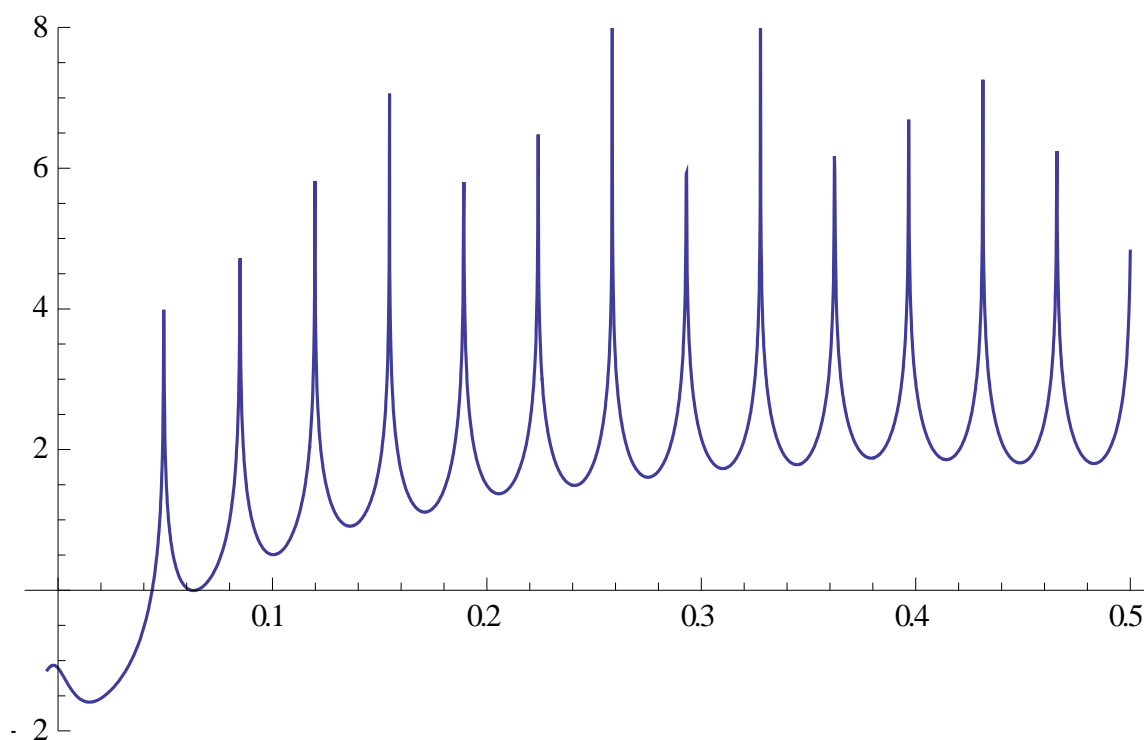


Figure 17: Structure factor for the sample pPS100-50.

6. Conclusion

The film formation of polystyrene colloids in ethanol solution was investigated for different concentrations and particle sizes. The optical microscope showed that for lower concentrations up to 20% (5mg/ml) a homogeneous thin film was formed. At intermediate concentrations clusters of increasing size appeared on top of the film and at higher concentrations from 75% (18.75 mg/ml) a continuous thick film was present. For the colloids with carboxylated surface the formation of cone-shaped structures on top of the film was observed, beginning at 20% (5 mg/ml) concentration.

The analysis of the X-ray images yielded a typical length scale near the colloid sizes, 91 ± 9 nm for the 100 nm particles and 188 ± 34 nm for the 200 nm particles. Whether the distances found from the additional peak near the central maximum have a physical meaning as such is not clear. The fact that they are similar (250 ± 50 nm for 100 nm colloids and 275 ± 70 for 200 nm colloids) for different sized particles speaks against the explanation of small clusters formed by only a few particles.

Higher order peaks were observed at lower concentrations (10% and 50%), but not at higher concentration (75% and 100%). An explanation for this can be the different incident beam angle which was higher for the higher concentrations resulting in less surface sensitivity.